Characterization of Two Polymorphs of Salmeterol Xinafoate Crystallized from Supercritical Fluids

Henry H. Y. Tong,[1] Boris Yu. Shekunov,[2,3] Peter York,[2,3] and Albert H. L. Chow[1,4]

Received January 16, 2001; accepted March 6, 2001

Purpose. To characterize two polymorphs of salmeterol xinafoate (SX-I and SX-II) produced by supercritical fluid crystallization.

Methods. SX-I and SX-II were crystallized as fine powders using Solution Enhanced Dispersion by Supercritical Fluids (SEDS). The two polymorphs and a reference micronized SX sample (MSX) were characterized using powder X-ray diffractometry (PXRD), Fourier transform infrared spectroscopy (FTIR), differential scanning calorimetry (DSC), thermogravimetric analysis (TGA), aqueous solubility (and dissolution) determination at 5–40°C, BET adsorption analysis, and inverse gas chromatography (IGC).

Results. Compared with SX-I, SX-II exhibited a lower enthalpy of fusion, a higher equilibrium solubility, a higher intrinsic dissolution rate, a lower enthalpy of solution (based on van't Hoff solubility plots), and a different FTIR spectrum (reflecting differences in intermolecular hydrogen bonding). Solubility ratio plot yielded a transition temperature (~99°C) below the melting points of both polymorphs. MSX showed essentially the same crystal form as SX-I (confirmed by PXRD and FTIR), but a distinctly different thermal behaviour. Mild trituration of SX-I afforded a similar DSC profile to MSX while prolonged grinding of SX-I gave rise to an endotherm at ~109°C, corresponding to solid-solid transition of SX-I to SX-II. Surface analysis of MSX, SX-I, and SX-II by IGC revealed significant differences in surface free energy in terms of both dispersive (nonpolar) interactions and specific (polar) acid-base properties.

Conclusions. The SEDS-processed SX-I and SX-II display high polymorphic purity and distinctly different physical and surface properties. The polymorphs are related enantiotropically with SX-I being the thermodynamically stable form at room temperature.

KEY WORDS: supercritical fluid crystallization; salmeterol xinafoate polymorphs; physical properties; solubilities; surface energetics; polymorphic purity.

INTRODUCTION

The development of cost-efficient technologies for producing consistent drug powders with the desired physicochemical properties for processing and formulation into inhalation products continues to pose challenges to pharmaceutical manufacturers. Conventionally, drug powders formulated for the inhalation route are produced by batch crystallization from a suitable solvent followed by micronization (fluid energy milling) to the appropriate particle size range (1–5 μm) for deep lung delivery. However, such a two-step approach is often time-consuming and costly, and the micronization process involved may render the resulting materials highly charged, cohesive, and difficult to process down-stream, and can even generate metastable solid phases and amorphous micro-domains, leading to reduced stability and increased susceptibility to moisture.

In recent years, supercritical fluid technologies have gained increasing attention in the pharmaceutical industry due to their capability and versatility of producing micro-fine particles to predetermined specifications. The use of SCFs to process pharmaceutical materials has proved to be a cost-efficient approach in generating high purity, micron-sized particles with defined morphology in a single-step operation (1,2). The attractive physical properties of SCFs such as variable density and transport properties (e.g. viscosity and diffusivity), and the relative ease by which these properties can be manipulated with temperature and pressure have created tremendous formulation opportunities for engineering drug particles with specific biological applications. Of all the SFC techniques reported, the SEDS (Solution Enhanced Dispersion by Supercritical Fluids) process has shown particular promise. In a single step operation, the technique is capable of producing micron-sized particles that are solvent-free, crystalline, and within a narrow size range, and the particle properties can be controlled simply by varying the processing parameters. In addition, the SEDS process can be used to regulate the crystal form of the particles by providing the appropriate conditions of temperature and pressure for the formation of the thermodynamically stable form. As a demonstration of this processing capability, the present study has examined the production of two polymorphic forms of salmeterol xinafoate by the SEDS technology. In particular, the physical and surface characteristics of these polymorphs have been investigated using powder X-ray diffraction (PXRD), Fourier transform infrared spectroscopy (FTIR), differential scanning calorimetry (DSC), thermogravimetric analysis (TGA), solubility determination, and inverse gas chromatography (IGC).

Salmeterol xinafoate (4-hydroxy-α^1-[[[6-(4-phenylbutoxy)hexyl]amino]methyl]-1,3-benzenedimethanol, 1-hydroxy-2-naphthalenecarboxylate) (SX) is a highly selective long-acting beta$_2$-adrenergic bronchodilator (3). SX is known to exist in two crystalline polymorphic forms with Form I (SX-I) being the stable and Form II (SX-II) the metastable polymorph under ambient conditions (4,5). Commercial SX is a micronized form (MSX) with essentially the same crystal structure of SX-I, as determined by PXRD and DSC. However, the possibility that commercial MSX may contain traces of SX-II formed during the micronization process cannot be ruled out since routine analysis of the polymorphic purity of the sample is constrained by the low sensitivity (5%) of the PXRD and DSC techniques used. While SX-I can be readily obtained by conventional crystallization methods, formation of pure SX-II has thus far only been possible with the SEDS techniques (4,5). The primary objective of the present investigation was to characterize the material and surface properties of the SEDS-processed SX-I and SX-II polymorphs, with

[1] School of Pharmacy, The Chinese University of Hong Kong, Shatin, N.T., Hong Kong SAR, China.
[2] Bradford Particle Design p1c, 69 Listerhills Science Park, Campus Road, Bradford BD7 1HR, United Kingdom.
[3] Drug Delivery Group, School of Pharmacy, University of Bradford, Bradford BD7 1DP, United Kingdom.
[4] To whom correspondence should be addressed at School of Pharmacy, The Chinese University of Hong Kong, 6/F, Rm 616, Basic Medical Sciences Building, Shatin, New Territories, Hong Kong SAR, China. (e-mail: albert-chow@cuhk.edu.hk)

0724-8741/01/0600-0852$19.50/0

a view to exploiting these properties in dry powder inhalation formulations. As a reference material for comparative assessment, a commercial MSX sample has been similarly characterized.

MATERIALS AND METHODS

Chemicals and Reagents

Salmeterol free base and its xinafoate salt (drug standards), micronized salmeterol xinafoate (MSX) and raw material for powder production were a generous donation from GlaxoWellcome, Ware, UK. 1-hydroxy-2-naphthoic acid of ultra-pure grade was purchased from Aldrich, USA. HPLC grade methanol and acetonitrile and all analytical grade liquid probes used in IGC were purchased from Labscan, Germany. Analytical grade triethylamine and phosphoric acid (85%) were obtained from Riedel-del Haen, Germany. All water used was double distilled.

Production of Salmeterol Xinafoate Polymorphs (SX-I and SX-II) by the SEDS Process

The SEDS method (6,7) was employed to crystallize SX-I and SX-II from methanol solution. The method is based on very rapid mixing between supercritical CO_2, used as an antisolvent, and solution using a twin-fluid nozzle. This provides an efficient way for intensive mass-transfer and fast nucleation. The particle formation vessel (0.5 L volume) with the nozzle was placed in an air-heated oven. Pressure in the vessel was controlled by air-actuated back-pressure regulator (Tescom, 26-1700 with ER3000 electronic controller, Tescom Co., Elk River, MN, USA) and kept constant at 250 ± 1 bar. The difference in the inlet and outlet pressure was typically within 1% of its absolute value. Solution flow rate provided by a metering pump (Jasco PU-980, Jasco Co., Tokyo, Japan) was 0.12 L/hour. The CO_2 flow, supplied by a water-cooled diaphragm pump (Dosapro, Milton Roy, Pont-Saint-Pierre, France) was constant at 2000 NL/hour. Solution concentration of SX was 4.5% w/v. The temperature in the vessel was monitored by a thermocouple and defined the polymorphic form produced: SX-I was obtained at 40°C and SX-II at 90°C. At the end of the experimental run, the powders were dried using pure CO_2. Typical quantity of a material collected in the vessel was about 15 g.

Powder X-Ray Diffractometry

Powder X-ray diffraction patterns were recorded on a Philips Powder X-Ray Diffraction System, Model PW 1830 3kW (Phillips, Lelyweg, The Netherlands) using Cu anode (λ = 1.540562 Å) over the 2θ interval 2.0° to 40.0°. Step size was 0.02° with a counting time of 2 seconds.

Thermogravimetric Analysis (TGA)

TGA was performed in an open pan using a Perkin Elmer Thermogravimetric Analyzer TGA 7 with Thermal Analysis Controller TAC 7/DX (Perkin Elmer, CT, USA).

Differential Scanning Calorimetry (DSC)

DSC profiles were generated using a Perkin Elmer Pyris 1 differential scanning calorimeter (with Pyris Manager software) (Perkin Elmer, CT, USA). Indium (T_m = 156.6°C; ΔH_f = 28.45 J g^{-1}) was used for routine calibration. Accurately weighed samples (1.0–1.5mg) were placed in hermetically sealed aluminium pans. Scanning speeds ranging from 2°C min^{-1} to 40°C min^{-1} were employed and the data collected at 10°C min^{-1} were used for quantitation.

Hot Stage Microscopy

The samples were examined under a hot stage microscope (Leica Galen III) for the melting and recrystallization events. Heating rate was set at 10°C min^{-1}.

Fourier-Transform Infrared Red Spectroscopy

Spectra were recorded from KBr disks using a Perkin-Elmer Fourier-Transform Infrared Red System (SpectrumBX) (Perkin-Elmer Beaconsfield, Buckinghamshire, UK). Number of scan was 16 and resolution was 4 cm^{-1}. The samples were scanned from 4000 to 400 cm^{-1} at an interval of 2 cm^{-1}.

Specific Surface Area Determination

Specific surface area was determined by BET nitrogen adsorption using a Surface Area Analyzer (Coulter SA 3100, Miami, FL, USA). Samples were placed in glass sample holders and outgassed with helium (purity > 99.999%) at 40°C for 16 h before analysis. Nitrogen (purity > 99.999%) was used as adsorbate and BET surface area was recorded as specific surface area of the samples. All measurements were performed in triplicate.

Dissolution Rate Measurement

25 ± 0.1mg of the sample were put in 150ml water in airtight amber glass bottle in a shaking water bath (Shaker Bath SBS30, Tilling Drive Stone, Staffordshire, UK) protected from light. Temperature was controlled at 25.0 ± 0.1°C and speed set at 100 revs min^{-1}. At appropriate time intervals, aliquots were withdrawn, filtered with 0.22 μm membrane filters, and diluted with a suitable amount of methanol prior to UV measurement at 280 nm (Spectronic GeneSys 5). The calibration curves in all analyses were linear ($r^2 > 0.999$). At the end of each dissolution run, the crystals remaining in solution for the SX-II samples were harvested from the mother liquors, dried on filter paper, and checked for polymorphic conversion by DSC. The intrinsic dissolution rate (i.e. initial dissolution rate divided by surface area determined by BET adsorption) was calculated for each crystal sample. Triplicate measurements were taken.

Equilibrium Solubility Determination

Equilibrium solubility of SX in water was determined in the temperature range of 5°C to 40°C. Stability studies using HPLC showed negligible degradation of SX in water within the temperature range (5–40°C) and the time period employed (3–5 days). However, SX was sensitive to light and chemical decomposition was significant above 50°C. Thus, the samples and the water-bath in which they were kept were fully covered to protect from light throughout the course of the study, and solubility determination was limited to 40°C. All temperatures were controlled within ± 0.1°C. 10.0 ± 0.1 mg of SX were placed in airtight (screw-capped) test tubes containing 8 ml of water. Studies at 25°C to 40°C were conducted in a thermostatic shaking water bath (Shaker Bath SBS30) for 3 days while experiments at 5°C to 25°C were carried out in a refrigerated bath (Refrigerated Circulating

Polyscience 9105, Niles, IL, USA) for 5 days. For experiments conducted at above-ambient temperatures, the pipette tips used were pre-warmed to prevent crystallization during aliquot withdrawal. The aliquots were assayed for SX by UV spectroscopy, and the SX-II crystals harvested at the end of each run were checked for polymorphic conversion by DSC as described before. Data were discarded if polymorphic change was evident in DSC.

High Performance Liquid Chromatography

HPLC analysis followed that reported in the literature with slight modification (8). The analysis was performed using a Hewlett Packard Series 1050 HPLC system (Waldbronn, Germany), a 250 × 4.6mm Hypersil 5μm C18 ODS column, (Welwyn Garden City, Herfordshire, UK) and a UV detector set at 225 nm. The mobile phase, composed of methanol, water, acetonitrile, phosphoric acid (85% v/v), and triethylamine (mixed in volume ratio of 55:35:10:0.1:0.1) was eluted isocratically at a flow rate of 1.2 ml min^{-1}. The sample was eluted as two peaks at retention times of 9.12 min and 14.93 min, corresponding to 1-hydroxy-2-naphthoic acid and salmeterol base respectively. SX was quantitated in terms of the area of the second peak (i.e salmeterol base), and excellent linearity was obtained for the standard calibration curves (r^2 > 0.9999).

Inverse Gas Chromatography (IGC)

IGC was performed on a Hewlett Packard Series II 5890 Gas Chromatograph (Wilmington, DE, USA) equipped with an integrator and flame ionization detector. Injector and detector temperatures were maintained at 100°C and 150°C respectively. Glass columns (60 cm long and 3.5 mm i.d.) were deactivated with 5% solution of dimethyldichlorosilane in toluene before being packed with SX powder. The columns were plugged with silanised glass wool at both ends and maintained at 40°C. Data were obtained for a known weight and surface area of the sample using a nitrogen gas (purity > 99.995%) flow of 20 ml min^{-1}. The column was weighed before and after the experiment to ensure no loss of materials during the run. Trace amount of vapour from non-polar and polar probes was injected. The retention times and volumes of the injected probes were determined at infinite dilution and thus were independent of the quantity of probes injected. The non-polar probes employed were pentane, hexane, heptane, octane, and nonane; the polar probes were dichloromethane, chloroform, acetone, ethyl acetate, tetrahydrofuran, and diethyl ether. Triplicate measurements in separate columns were made.

RESULTS

Powder X-Ray Diffraction (PXRD)

SX-I and SX-II showed different X-ray diffraction patterns. SX-I was characterized by a sharp peak at 2θ = 4.158° and multiple sharp peaks at 2θ = 9°–26° while SX-II exhibited a sharp peak at 2.853°, and a few relatively indistinct peaks at 9° to 26° (Fig. 1) indicative of marked structural differences between the two forms.

MSX displayed essentially the same XRPD pattern as SX-I (Fig. 1). Maintaining the sample at 130°C in a mounted heating cell yielded a diffraction pattern characteristic of the SX-II structure only. This is consistent with a polymorphic conversion from SX-I to SX-II.

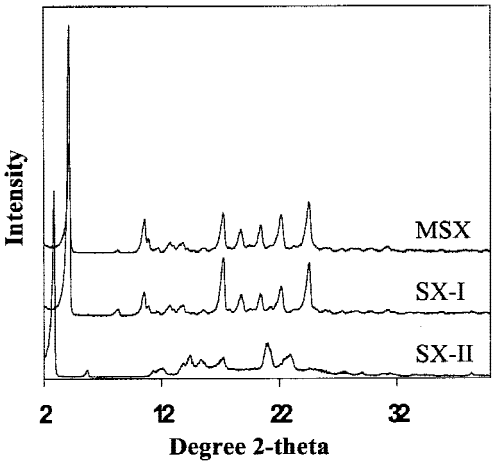

Fig. 1. Powder X-ray diffraction patterns of MSX, SX-I, and SX-II.

FTIR Spectroscopy

The FTIR spectra of MSX resembled closely those of SX-I (Fig. 2). However, distinct spectral differences were observed between SX-I and SX-II over almost the whole fingerprint region. In addition, there was an obvious band shift in the stretching region of OH (at 3308cm^{-1} for SX-I and at 3426, 3294cm^{-1} for SX-II) and NH (marked by differences in shape and size of the broad peak at 3000-2273cm^{-1}) (9). This indicates a significant difference in intermolecular hydrogen bonding network between the two polymorphs.

Thermal Gravimetric Analysis (TGA), Differential Scanning Calorimetry (DSC), and Hot Stage Microscopy (HSM)

TGA revealed no significant weight loss of the samples until the temperature reached 150°C, at which solid-state decomposition became evident. This suggests an absence of solvated forms and negligible adsorption of moisture on the samples.

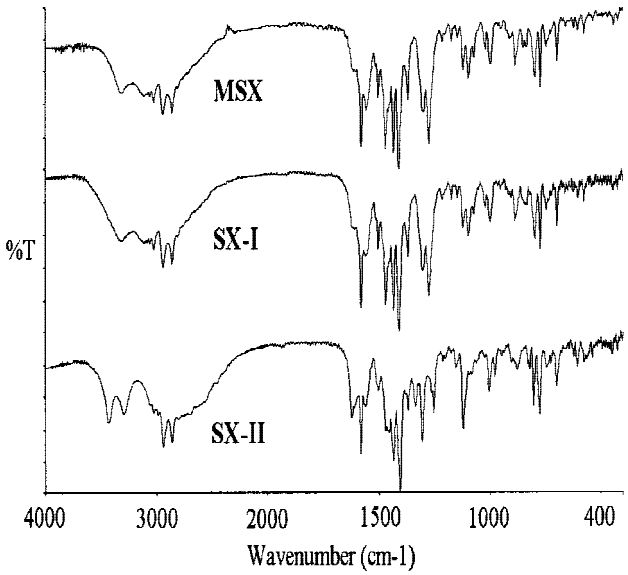

Fig. 2. FT-IR spectra of MSX, SX-I, and SX-II in the range of 4000–400cm^{-1}.

DSC analysis afforded a single melting endotherm at 137.6°C (ΔH_f = 42.02 kJ mol^{-1}) for SX-II and a large endotherm at 122.7°C (ΔH_f = 68.29 kJ mol^{-1}) followed by a small endotherm at 137.6°C for SX-I (Fig. 3A). HSM confirmed similar thermal events. Increasing the DSC scanning rate from 10°C min^{-1} to 40°C min^{-1} eliminated completely the small endotherm at 137.6°C for SX-I, whereas lowering the scanning speed to 5 or 2°C min^{-1} tended to accentuate the size of this peak, and to give rise to a recrystallization exotherm immediately after the melting endotherm of SX-I at 122.7°C (Fig. 3C). In contrast, MSX showed a melting endotherm at 122.7°C followed immediately by a large recrystallization exotherm and a large melting endotherm at 137.6°C (Fig. 3B). Higher heating rate tended to reduce the size of the endotherm at 137.6°C. All these observations suggest that MSX undergoes polymorphic transformation upon heating more readily than does SX-I. This difference in rate of polymorphic conversion may be attributable to the presence of trace SX-II seeds in the MSX sample possibly formed during the micronization process (4,5). As a means for verification, the SX-I sample was further analyzed by DSC after being triturated for a defined period (i.e. 10 or 30 minutes) or physically mixed with ~5% SX-II. At a scanning speed of 10°C min^{-1}, the mildly triturated SX-I sample (i.e. triturated for 10 minutes) yielded a similar DSC curve to MSX (Fig. 3A), whereas the seeded sample showed minor changes in thermal behaviour (i.e. presence of a small exotherm for SX-II crystallization) compared with the unseeded or unground SX-I sample. This suggests that the physically mixed seeds of SX-II are less effective than those SX-II nuclei formed within SX-I by grinding for inducing the crystallization of SX-II from the SX-I melt. The more rapid recrystallization observed with SX-II nuclei may be explained by the close contact of the nuclei with the melting SX-I at the molecular level. However, for the vigorously ground sample (i.e. ground for 30 minutes), neither the melting peak of SX-I nor the recrystallization exotherm for SX-II formation was discernable; instead, a new endotherm at ~109°C emerged, followed by the characteristic melting endotherm of SX-II at ~138°C. This new endotherm probably corresponds to the solid-solid phase transition of SX-I to SX-II. In addition, the PXRD pattern of the SX-I sample remained essentially unchanged (i.e. with slight peak broadening only) after prolonged grinding. Thus, it would appear that the grinding treatment per se cannot bring about gross structural modification of SX-I, but can promote the solid-solid transition (i.e. molecular rearrangement) of SX-I to SX-II at the transition temperature (by reducing the activation energy required) without the need to go through the melting phase of SX-I at a higher temperature, as would be the case for the unground sample.

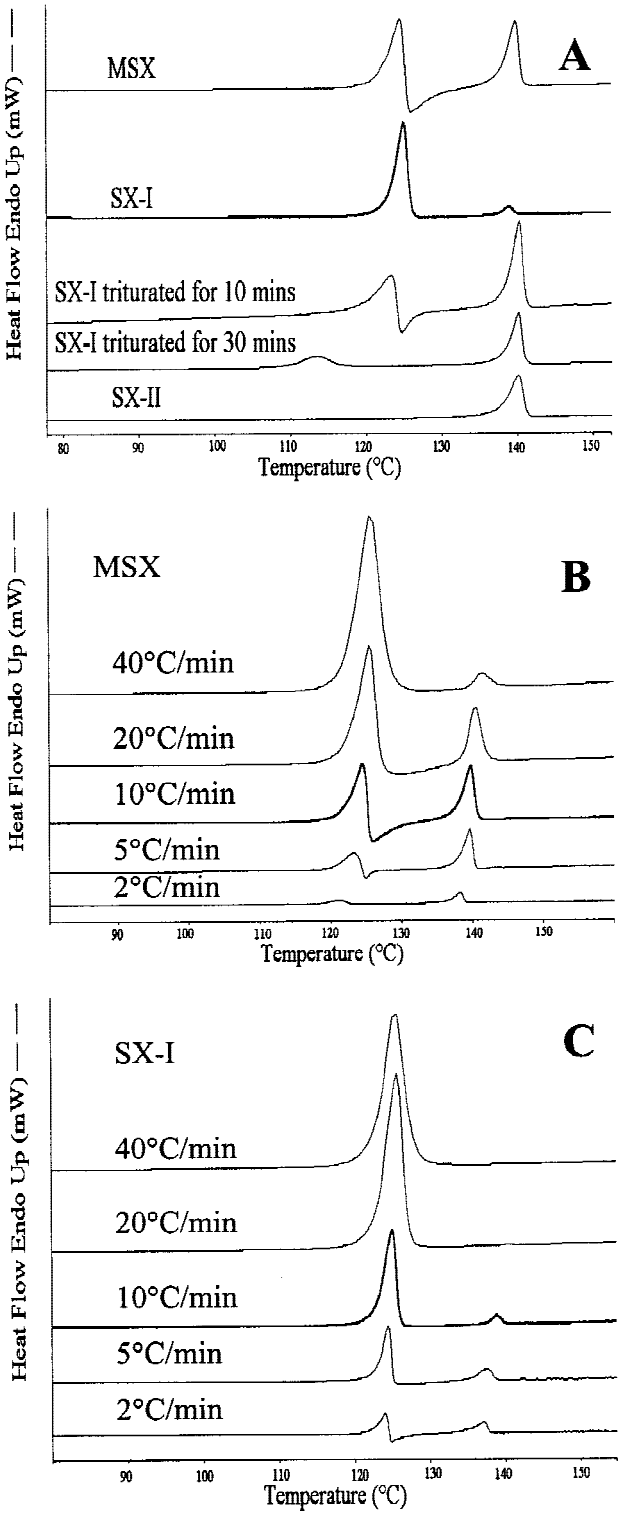

Fig. 3. DSC profiles of various SX samples: MSX, SX-I, SX-I triturated for 10 and 30 min, and SX-II at 10°C min^{-1} (A); MSX at 40, 20, 10, 5, and 2°C min^{-1} (B); SX-I at 40, 20, 10, 5, and 2°C min^{-1} (C).

Powder Dissolution Studies

MSX and SX-I powders displayed similar dissolution profiles at 25°C (Fig. 4). SX-II (b; n = 2) maintained a consistently higher concentration in water than either MSX or SX-I throughout the whole study period and retained its original physical structure, as confirmed by DSC. However, SX-II (a; n = 1) was converted to SX-I after one week, resulting in a decrease in solubility.

Based on the Noyes-Whitney equation (10), the intrinsic dissolution rate (ITR) of the SX powdered samples under sink conditions was calculated by dividing the initial dissolution rate (IDR; estimated from the initial slope of the dissolution curve within the first 30 minutes) by the surface area (determined by BET nitrogen adsorption) of the powders. The BET surface area and ITR data are tabulated in Table I.

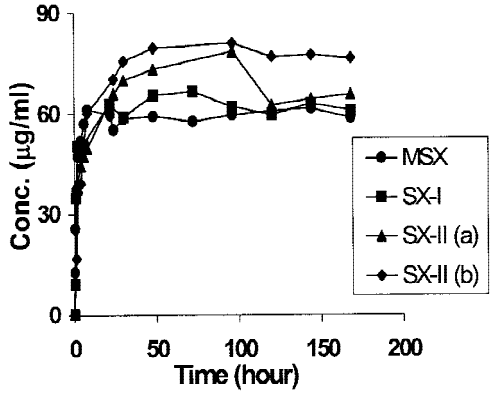

Fig. 4. Dissolution-time profiles of MSX, SX-I, and SX-II (a) (with polymorphic conversion) and SX-II (b) (without polymorphic conversion) in water at 25°C.

The IDRs were similar among MSX, SX-I, and SX-II, based on their dissolution profiles. However, the ITR (i.e. dissolution rate corrected for the effect of surface area) was the highest for SX-II while SX-I and MSX had comparable ITRs.

Equilibrium Solubility Studies

The solubility data at various temperatures were analyzed by the van't Hoff solubility-temperature plots. The results for SX-I (n = 27) and SX-II (n = 25) are shown in Fig. 5A. As revealed by DSC, two of the SX-II samples underwent polymorphic conversion to SX-I, and these data were therefore excluded from the analysis. Backward extrapolation of the two linear plots yielded a transition temperature, T_t, of ~99°C for the two polymorphs. The solubility-temperature behaviours of MSX and SX-I were very similar although SX-I appeared to have a marginally higher solubility than MSX.

The enthalpy of polymorphic transition from SX-II to SX-I, $\Delta H_{II \to I}$, can be estimated from the slope of the plot of the logarithm of the solubility ratio of SX-II to SX-I (i.e. $\ln(X_{bII}/X_{bI})$) against the reciprocal of absolute temperature (i.e. 1/T) (Fig. 5B) (11,12). Since $X_{bII} = X_{bI}$ at the transition temperature (T_t = 98.3°C or 371.45K when $\ln(X_{bII}/X_{bI} = 0)$, the entropy of transition, $\Delta S_{II \to I}$, can be calculated from the relationship, $\Delta H_{II \to I} = T_t \Delta S_{II \to I}$ (i.e. when $\Delta G_{II \to I} = 0$). The calculated $\Delta H_{II \to I}$ and $\Delta S_{II \to I}$ are −4551 J mol^{-1} and −12.3 J K^{-1} mol^{-1} respectively. The free energy of transition, $\Delta G_{II \to I}$, at 25°C and 37°C can be similarly calculated from the equation, $\Delta G_{II\ to\ I} = \Delta H_{II \to I} - T\Delta S_{II \to I}$, yielding values of −884 J K^{-1} mol^{-1} and −736 J K^{-1} mol^{-1} respectively.

Inverse Gas Chromatography (IGC)

The fundamental quantity of inverse gas chromatography is the net retention volume, V_N, which is determined from (13,14):

$$V_N = j\ F\ (t_r - t_o) \quad (1)$$

where t_r is the retention time of a given probe, t_o is the zero retention reference time (void volume), F is the carrier flow rate, and j is a correction factor taking into account gas compressibility.

Adsorption of the probe molecules on solid surfaces can be considered in terms of both dispersive and specific components of surface free energy, corresponding to non-polar and polar properties of the surface. By virtue of their chemical nature, non-polar probes of the alkane series only have dispersive component of surface free energy, which can be determined from the slope of the plot based the following equation (13,14).

$$RT \ln V_N = 2\ a\ N\ (\gamma_S^D)^{1/2}(\gamma_L^D)^{1/2} + \text{constant} \quad (2)$$

where R is gas constant, T is the column's absolute temperature, a is the probe's surface area, *N* is Avogadro's number, γ_S^D is the dispersive component of surface free energy of solid (SX in this case) and γ_L^D is the dispersive component of surface free energy of the liquid probes.

Polar probes have both dispersive and specific components of surface free energy of adsorption. The specific component of surface free energy of adsorption (ΔG_A^{SP}) can be estimated from the vertical distance between the alkane reference line and the polar probes of interest. This free energy term can be related to the donor number (DN) and acceptor number (AN) of the polar by the equation (Eq. 3) shown below. DN defines the basicity or electron donor ability of a probe whilst AN defines the acidity or electron acceptor ability. In practice, the quantity AN* is often used in place of AN since it is corrected for the contribution of the dispersive component to AN (15–17).

Assuming that the entropic contribution is negligible, $-\Delta G_A^{SP}$ was used instead of $-\Delta H_A^{SP}$ to calculate the acid (K_A) and base (K_D) parameters of SX (17,18):

$$-\Delta G_A^{SP} = K_A\ DN + K_D\ AN^* \quad (3)$$

Plotting $-\Delta G_A^{SP}/AN^*$ against DN/AN* will yield a straight line where K_A and K_D correspond to the slope and intercept respectively.

The IGC data for the various SX samples were analyzed by the above approach, and the results are summarized in Table II.

DISCUSSIONS

Crystal Structures of MSX, SX-I, and SX-II

It has been reported that SX materials obtained by conventional crystallization invariably exist in the Form I structure (4,5). The present study demonstrates that while the MSX sample possesses the crystal structure of Form I, it is more prone to polymorphic conversion than the SEDS SX-I powder above the transition temperature, as evidenced by DSC. This indicates that the micronization process employed for particle size reduction might have generated SX-II nuclei and amorphous micro-domains in MSX, thereby giving rise to more rapid polymorphic transformation (4). On the other hand, the SEDS SX-I sample, being devoid of Form II seeds, has a higher activation energy barrier against polymorphic conversion, and its transformation to SX-II, therefore, occurs more slowly. This inference has been further substantiated by the observation that mildly ground SX-I sample displayed similar DSC profile to MSX while vigorously ground sample yielded a solid-solid phase transition of SX-I to SX-II at ~109°C. The SEDS SX-II also demonstrates a significant resistance to polymorphic conversion to SX-I under ambient conditions (i.e. below the transition point). Storage of the SX-II sample at room temperature and relative humidity over

Table I. Aqueous Solubilities, Specific Surface Areas and Dissolution Rates of MSX, SX-I, and SX-II

Sample	Initial dissolution rate ($\mu g\ ml^{-1}\ hr^{-1}$)	Solubility ($\mu g\ ml^{-1}$)	Intrinsic dissolution rate constant ($cm\ sec^{-1}$) $\times 10^5$	Specific surface area ($m^2\ g^{-1}$)	Intrinsic dissolution rate ($\mu g\ min^{-1}\ cm^{-2}$)
MSX	51.14	61.70	1.648	8.382	0.061
SX-I	34.78	66.82	1.445	6.003	0.058
SX-II	24.15	81.07	4.366	1.137	0.212

a period of 2 years showed no discernable polymorphic changes and solubility studies at 25–40°C over a period of 3–5 days also revealed excellent physical stability. In addition, prolonged trituration of SX-II resulted in a reduction of crystallinity of the material, but no apparent polymorphic conversion, as confirmed by DSC and PXRD. All these observations would strongly suggest that the SEDS process is capable of producing SX-I and SX-II in highly pure forms (i.e. free from the nuclei of the alternative form), which has not been achievable with conventional crystallization techniques.

Enantiotropic Pair of SX-I and SX-II

Burger and Ramberger have established useful thermodynamic rules for determining whether a system is enantiotropic or monotropic based on thermodynamic measurements. The heat (or enthalpy) of fusion rule states that if the higher melting form has the lower heat of fusion then the two forms are related enantiotropically, otherwise they are monotropic (19,20). As determined by DSC, SX-I has a T_m of 122.7°C and a ΔH_f of 68.29 kJ mol^{-1} while the T_m and ΔH_f of SX-II are 137.6°C and 42.02 kJ mol^{-1} respectively. Accordingly, the two polymorphs are related enantiotropically.

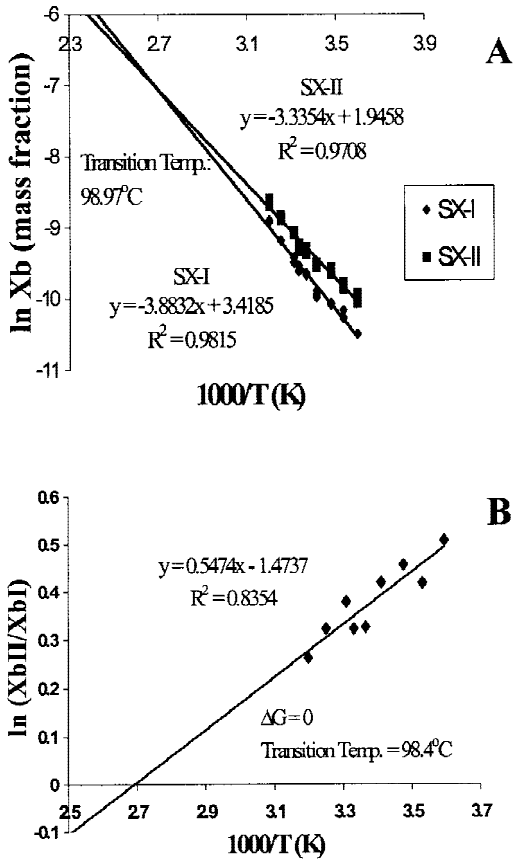

Fig. 5. Van't Hoff plots of log solubility (A) and log solubility ratio (B) for SX-I and SX-II as a function of the reciprocal of absolute temperature.

Dissolution and solubility studies showed that SX-II has a higher ITR, higher equilibrium solubility in water, and higher negative Gibb's free energy of solution (at 5–40°C) than SX-I. Thus, SX-II is the less stable form under ambient conditions which is consistent with the general thermodynamic rules for metastable polymorph (12). The transition temperature (T_t) estimated from the van't Hoff solubility-temperature plot is well above ambient temperature but lower than the melting point (T_m) of both SX-I and SX-II, which is consistent with enantiotropic polymorphism. As discussed earlier, the equilibrium solubility measurements were confined to temperatures below 40°C to avoid chemical degradation, and only the data obtained within the temperature range of 5–40°C could be used to estimate T_t by extrapolation. As has been well documented, extrapolation of data 10K beyond the experimental range is prone to produce considerable errors and is not reliable (21). In addition, such linear extrapolation assumes that ΔH_s and ΔC_p are independent of temperature throughout the temperature range of interest, which is unlikely to hold for extrapolation spanning almost 60K in the present case. Thus, the T_t (~99°C) obtained can at best be viewed as an approximate estimate.

As noted earlier, the T_t for the two polymorphs can also be estimated from the DSC curve of vigorously ground SX-I sample. The observed T_t in DSC (~109°C) differs from that determined from van't Hoff solubility plots by about 10°C. This discrepancy is perhaps not surprising, considering the fact that neither technique is free from limitations or drawbacks. The solubility method has both experimental and theoretical constraints as already discussed while the accuracy of the DSC technique is limited by its dynamic nature and the material-dependent resistance to solid-solid phase transition at the transition temperature. Thermodynamics predicts that the solid-solid phase transition in question will occur once the transition temperature is reached. However, the expected phase transition of SX-I to SX-II can only be detected or effected after prolonged grinding of the sample, reflecting the complex interplay of kinetics and thermodynamics in the observed thermal behaviour of the sample.

As with the ΔH_f data, the enthalpy of solution, ΔH_s, of SX-I determined from the van't Hoff solubility plot (32.29 kJ mol^{-1}) was higher than that of SX-II (27.73 kJ mol^{-1}), further substantiating SX-II as the thermodynamically stable form at room temperature. However, the difference in ΔH_f (at T_m) values between SX-I and SX-II was much higher than that of ΔH_s (determined at room temperature), which is attributed to a large difference in the molar heat capacity, ΔC_p, between the two crystal forms (12).

Table II. Surface Thermodynamic Properties of MSX, SX-I, and SX-II Determined at 40°C by IGC[a]

Sample	γ_S^D mJm^{-2}	$-\Delta G_A^{sp}$ kJ mol^{-1}						Acid and base parameters	
		Dichloromethane	Chloroform	Acetone	Ethyl acetate	Diethyl ether	Tetrahydrofuran	K_A	K_D
MSX	38.285	—	0.810	4.560	3.995	2.774	3.609	0.172	0.298
	(0.907)		(0.053)	(0.096)	(0.013)	(0.041)	(0.027)	(0.001)	(0.021)
SX-I	32.476	2.808	0.153	3.797	2.705	1.488	2.446	0.110	0.356
	(0.254)	(0.147)	(0.080)	(1.173)	(0.613)	(0.390)	(0.279)	(0.013)	(0.120)
SX-II	28.557	6.108	4.502	4.472	4.018	1.863	4.417	0.191	0.554
	(1.108)	(0.166)	(0.125)	(0.146)	(0.109)	(0.060)	(0.135)	(0.006)	(0.013)

[a] Standard deviations are shown in parentheses.

Surface Properties of MSX, SX-I, and SX-II

Data from IGC demonstrated that the dispersive component of surface free energy, $_S^D$, of SX-II is smaller than that of SX-I while the acidity and basicity constants derived from the specific interactions, K_A and K_D, of SX-II are larger than those of SX-I (Table II). In addition, the specific component of surface free energy of adsorption, $-\Delta G_A^{SP}$, of SX-II is larger than that of SX-I for all the polar probes used. The relatively high surface free energy of SX-II may be ascribed to its proton donor groups (OH and COOH) and proton acceptor group (NH) being more exposed than the nonpolar bulky groups (i.e. benzene and naphthalene) at the crystal surface. Further studies employing molecular modelling are necessary to verify this point.

While MSX and SX-I possess identical crystal structure, MSX displays a larger γ_S^D and a larger $-\Delta G_A^{SP}$ (for all the polar probes) than SX-I. This is perhaps not unexpected since micronization is known to augment surface free energy by introducing surface structural defects and possibly by increasing the proportion of the polar faces.

CONCLUSION

The two polymorphs of SX (SX-I and SX-II) produced in a controlled one-step operation by the SEDS technology exhibit high polymorphic purity, as suggested by their relative resistance to solid phase transition under thermodynamically favorable conditions. Solubility and DSC studies confirm that these polymorphs are enantiotropes with the SX-I being the thermodynamically stable form at room temperature. Compared with MSX, the SEDS-processed SX-I material is a more stable physical form, as reflected by their differences in thermal and surface properties.

ACKNOWLEDGMENTS

Financial support from the Chinese University of Hong Kong (Special Grant for conducting research abroad in summer) and the Research Grant Council of Hong Kong (Earmarked Grant CUHK4244/98M) is gratefully acknowledged.

REFERENCES

1. B. Y. Shekunov and P. York. Crystallization processes in pharmaceutical technology and drug delivery design. *J. Crystal Growth* **211**:122–136 (2000).
2. S. Palakodaty and P. York. Phase behavioral effects on particle formation processes using supercritical fluids. *Pharm. Res.* **16**: 976–985 (1999).
3. Serevent® (salmeterol xinafoate) Inhalation Aerosol Product Information, Glaxo Wellcome Inc, 1998.
4. P. York, M. Hanna and G. O. Humphreys. Crystal Engineering and Particle Design for Drug Delivery Systems Using Supercritical Fluid Technologies. *Proceedings of the Asian Conference and Exhibition on Controlled Release*, Controlled Release Society, Inc., 1999 pp. 134–135.
5. S. Beach, D. Latham, C. Sidgwick, M. Hanna, and P. York. Control of the Physical Form of Salmeterol Xinafoate. *Org. Proc. Res. & Dev.* **3**:370–376 (1999).
6. P. York and M. Hanna. Particle engineering by supercritical fluid technologies for powder inhalation drug delivery. *Proceedings of the Conference on Respiratory Drug Delivery,* Phoenix, 1996 V: 231–239.
7. B. Yu. Shekunov, M. Hanna, and P. York. Crystallization process in turbulent supercritical flows. *J. Crystal Growth* **198/199**:1345–1351 (1999).
8. V. G. Nayak, S. G. Belapure, C. D. Gaitonde, and A. A. Sule. Determination of salmeterol in metered-dose and dry-powder inhalers by reversed-phase high performance liquid chromatography. *J. Pharm. Biomed. Anal.* **14**:511–513 (1996).
9. R. M. Silverstein, G. C. Bassler, and T. C. Morrill. *Spectrometric Identification of Organic Compounds (5th edition)*, John Wiley & Sons Inc, New York, 1991.
10. A. Noyes and W. Whitney. The rate of solution of solid substances in their own solutions. *J. Am. Chem. Soc.* **19**:930–934 (1897).
11. D. J. W. Grant, M. Mehdizadeh, A. H. L. Chow, and J. E. Fairbrother. Non-linear van't Hoff solubility-temperature plots and their pharmaceutical interpretation. *Int. J. Pharm.* **18**:25–38 (1984).
12. D. J. W. Grant and T. Higuchi. *Solubility Behavior of Organic Compounds*, John Wiley & Sons Inc, New York, 1989.
13. J. Schultz and L. Lavielle. Interfacial properties of carbon fiber-epoxy matrix composites. In D. R. Lloyd, T. C. Ward, H. P. Schreiber, and C. C. Pizana (eds.), *Inverse Gas Chromatography-Characterization of Polymers and Other Materials*, American Chemical Society, Washington, 1989 pp. 185–202.
14. J. Schultz, L. Lavielle, and C. Martin. The role of the interface in carbon fibre-epoxy resin composites. *J. Adhesion* **23**:45–60 (1987).
15. F. M. Fowkes. Quantitative characterization of the acid-base properties of solvents, polymers, and inorganic surfaces. *J. Adhesion Sci. Technol.* **4**:669–691 (1990).
16. V. Gutmann. *The Donor-Acceptor Approach to Molecular Interactions*, Plenum, New York, 1978.
17. J. C. Feeley, P. York, B. S. Sumby, and H. Dicks. Determination of surface properties and flow characteristics of salbutamol sulphate, before and after micronisation. *Int. J. Pharm.* **172**:89–96 (1998).
18. M. D. Ticehurst, R. C. Rowe, and P. York. Determination of surface properties of salbutamol sulphate by inverse gas chromatography. *Int. J. Pharm.* **111**:241–249 (1994).
19. A. Burger and R. Ramberger. On the polymorphism of pharmaceuticals and other molecular crystals. I. Theory of thermodynamic rules. *Mikrochim. Acta* **11**:259–271 (1979).
20. A. Burger and R. Ramberger. On the polymorphism of pharmaceuticals and other molecular crystals. II. Applicability of Thermodynamic rules. *Mikrochim. Acta* **11**:273–316 (1979).
21. S. R. Byrn, R. R. Pfeiffer, and J. G. Stowell. *Solid State Chemistry of Drugs (2nd edition)*, SSCI Inc, West Lafayette, Indiana, 1999.